J. Fluid Mech. (1996), vol. 318, pp. 251–271

Resonant gas oscillations exhibiting mixed nonlinearity

By E. A. COX[1] AND A. KLUWICK[2]

[1] Department of Mathematical Physics, University College Dublin, Belfield, Dublin 4, Ireland

[2] Institute of Fluid Dynamics and Heat Transfer, Technical University, Vienna, Austria

(Received 10 May 1995 and in revised form 17 February 1996)

A closed tube containing a BZT-fluid is driven by an applied velocity near and at resonant frequencies. A small-rate theory is shown to predict the existence of stable periodic expansion and compression shocks in a resonant frequency band. The significant effects of wave interaction and thermoviscous damping are demonstrated.

1. Introduction

There is a long history of studies dealing with the effects of mixed nonlinearity on one-dimensional waves with and without phase transition (for overviews see for example Kutateladze, Nakoryakov & Borisov 1987; Kluwick 1991; Dunn, Fosdick & Slemrod 1993). Probably the most exciting prediction of these studies is the existence of negative shocks, e.g. shocks across which the normal stress decreases. The possibility that negative shocks may form in real single-phase fluids seems to have been recognized first by Bethe (1942) and independently by Zel'dovich (1946) who also considered shock-induced phase changes. Here we are mainly concerned with propagation phenomena in single-phase equilibrium flows. The steepening characteristics of waves then are given by the nonlinearity parameter or fundamental derivative

$$\tilde{\Gamma} = \frac{1}{\rho}\frac{\partial(\rho a)}{\partial \rho}\bigg|_s .$$

Here ρ, a and s denote, respectively, the density, the speed of sound and the entropy.

Classical gasdynamics is based on the assumption of positive nonlinearity, e.g. that $\tilde{\Gamma}$ is a strictly positive quantity as in the case of perfect gases. However if, for example, $\tilde{\Gamma}$ changes sign on a transition line in the pressure–specific volume diagram, then the fluid exhibits mixed nonlinearity and the richness of the resulting wave dynamics increases significantly. So far two mechanisms which may cause $\tilde{\Gamma}$ to change sign in the neighbourhood of the thermodynamic critical point have been identified. The first is associated with the critical point singularity of the isochoric heat capacity c_v. The second rests on the result following from standard thermodynamics that isentropes and isotherms differ only slightly if the heat capacities of the fluid under consideration are large in general, e.g. if the fluid consists of complex molecules, see Thompson (1971), Thompson & Lambrakis (1973). In recognition of the significance of the studies by Bethe, Zel'dovich and Thompson, fluids of this latter type are now commonly referred to as BZT-fluids.

Thermodynamic considerations also indicate that fluids with large heat capacities may be ideal working fluids for organic Rankine cycles (Curran 1981; Zörner &

Blumenberg 1989). Studies dealing with the flow properties of such fluids have added further support to this prediction (Cramer & Best 1991; Cramer & Tarkenton, Kluwick 1993; Cramer & Fry 1993). As a result of these studies gasdynamic flows of BZT-fluids in the dense gas regime are fairly well understood theoretically.

Unfortunately, difficulties with the required high temperature and pressure levels have so far prevented the experimental verification of most theoretical results, in particular the existence of single-phase expansion shocks. Experiments carried out by Borisov *et al.* (1983) showing the formation of stable rarefaction waves clearly capture effects of negative nonlinearity caused by the critical point singularity of c_v. However, in these experiments the flow medium, Freon 13, appears to have entered the two-phase region. To the authors' knowledge corresponding experiments with single-phase BZT-fluids have not been performed yet.

Propagating shocks of (almost) constant strength can be generated in at least two ways, using shock tubes or resonance tubes. Shock tube experiments in the dense gas regime require highly sophisticated techniques and produce a discontinuous set of data but have the advantage of a relatively simple theoretical basis. Experiments in resonance tubes are expected to be much easier and by controlling the piston frequency it should be possible to vary the shock strength continuously over the interesting range of thermodynamic states. Moreover, owing to the smallness of the nonlinearity parameter in the neighbourhood of the transition line $\tilde{\Gamma} = 0$ relatively strong shocks can, in principle, be generated by applying moderate piston amplitudes. However, the theoretical interpretation of the results requires the investigation of interacting oppositely travelling waves and this is significantly more complicated than in the case of unidirectional waves occurring in shock tubes. Existing work deals with media having strictly positive nonlinearity only (Betchov 1958; Chester 1964, 1981; Jimenez 1973). In the present study the analysis is extended to include the effects of negative and mixed nonlinearity. This is certainly an interesting task in itself but it is hoped that the results will stimulate experimental research on resonant oscillations in the dense gas regime with the aim to conclusively show the existence of negative shock waves in single-phase BZT-fluids.

2. Problem formulation

A column of gas is contained in a pipe of length L. One end of the pipe is closed, and an oscillating piston is located at the other end. The pressure and density of the gas are measured from and non-dimensionalized with respect to the reference state (p_o, ρ_o) with associated sound speed a_o. The reference pressure is taken to be the mean of the time-periodic gas oscillation. We formulate the problem in terms of the non-dimensional variables $a_o v, \rho_o a_o^2 p, \rho_o \rho, Lx$ and $La_o^{-1}t$ where x is a Lagrangian coordinate labelling a material particle which in the reference state is a distance x from the closed end of the pipe.

The equations of momentum and mass conservation in Lagrangian form are

$$\frac{\partial v}{\partial t} + \frac{\partial p}{\partial x} = 0 \tag{2.1}$$

and

$$\frac{\partial}{\partial t}\left(\frac{1}{1+\rho}\right) - \frac{\partial v}{\partial x} = 0, \tag{2.2}$$

where pressure disturbances, particle velocity and density disturbances are denoted by the variables p, v and ρ respectively.

The above equations must be supplemented by appropriate one-dimensional shock jump conditions. If a shock front envelopes at time t a particle with Lagrangian coordinate $x = X(t)$ then the Lagrangian shock speed $\pm u$ satisfies

$$\pm u = \frac{\mathrm{d}X}{\mathrm{d}t} = -\frac{[v]}{[(1+\rho)^{-1}]} = \frac{[p]}{[v]}, \tag{2.3}$$

where u is positive and the sign of the term $\pm u$ indicates the direction of propagation. A jump in a variable ϕ at the passage of a shock is indicated by $[\phi] \equiv \phi_a - \phi_b$ where the subscripts a, b refer to conditions after and before a shock. For the problem under consideration the entropy jump across weak shocks is fourth order in the pressure jump and entropy changes may be assumed negligible (see Cramer & Kluwick 1984).

Long-time-periodic solutions to equations (2.1)–(2.3) are sought subject to appropriate boundary conditions. At the closed end of the pipe, $x = 0$, we impose the condition

$$v(0,t) = 0. \tag{2.4}$$

At $x = 1$, we assume a periodic piston displacement of the form $\mu h(\omega t)$ where $\mu (\ll 1)$ is the ratio of piston amplitude to pipe length and ω is the non-dimensional piston frequency, i.e. $h(\phi + 1) = h(\phi)$. Therefore on $x = 1$ we have

$$v(1,t) = \mu\omega h'(\omega t)\ . \tag{2.5}$$

Equations (2.1) and (2.2) can be written in the characteristic form

$$\mathrm{d}v \pm \frac{a}{1+\rho}\mathrm{d}\rho = 0 \tag{2.6}$$

and

$$\frac{\mathrm{d}x}{\mathrm{d}t} \mp a(1+\rho) = 0, \tag{2.7}$$

where the sound speed is $a = (\mathrm{d}p/\mathrm{d}\rho)^{1/2}$. The upper and lower signs define right-running and left-running characteristics $\beta =$ constant and $\alpha =$ constant respectively.

The dependence of the sound speed a on the density ρ can readily be expressed in terms of a Taylor expansion about the reference sound speed a_o. This yields

$$a(\rho) = 1 + (\Gamma - 1)\rho + \tfrac{1}{2}(\Lambda + 2)\rho^2 + O(\rho^3), \tag{2.8}$$

where the nonlinear coefficients Γ and Λ are given by

$$\Gamma = \frac{\rho_o}{a_o}\tilde{\Gamma}(\rho_o, s_o)\ , \quad \Lambda = \left.\frac{\partial\Gamma}{\partial\rho}\right|_{\rho=0}\ . \tag{2.9}$$

Here $\tilde{\Gamma}$ is the fundamental derivative, discussed in §1 . In order that the periodic reference state lies in the neighbourhood of the transition line $\tilde{\Gamma}(\rho_o, s_o) = 0$ we have assumed in (2.8) that $\Gamma = O(\rho) = o(1)$ and $\Lambda = O(1)$.

Insertion of (2.8) into the slope conditions (2.7) yields

$$\pm\frac{\mathrm{d}x}{\mathrm{d}t} = 1 + (\Gamma\rho + \tfrac{1}{2}\Lambda\rho^2) + O(\rho^3) \tag{2.10}$$

and we note that nonlinear effects only enter at $O(\rho^2)$. The problem remains now to integrate (2.6) and (2.10).

If the characteristic variables α and β are considered as independent variables then as shown by Lin (1954) and Fox (1955) secular growth terms in the solution can be

avoided. The appropriate expansions for v and ρ are then

$$v(\alpha,\beta;\epsilon) = \epsilon v_1(\alpha,\beta) + \epsilon^2 v_2(\alpha,\beta) + \ldots, \tag{2.11}$$

$$\rho(\alpha,\beta;\epsilon) = \epsilon\rho_1(\alpha,\beta) + \epsilon^2\rho_2(\alpha,\beta) + \ldots \tag{2.12}$$

with the x,t coordinates expanded as

$$x(\alpha,\beta;\epsilon) = x_0(\alpha,\beta) + \epsilon x_1(\alpha,\beta) + \epsilon^2 x_2(\alpha,\beta) + \ldots, \tag{2.13}$$

$$t(\alpha,\beta;\epsilon) = t_0(\alpha,\beta) + \epsilon t_1(\alpha,\beta) + \epsilon^2 t_2(\alpha,\beta) + \ldots \tag{2.14}$$

The perturbation parameter ϵ is the Mach number of the gas and its relationship to the imposed piston velocity will be determined later as part of the solution.

Substituting the expansions (2.8), (2.11), (2.12) into the compatibility conditions (2.6) and integrating one obtains

$$2\epsilon f(\beta) = v + \int^{\rho} \frac{a(s)}{1+s}\mathrm{d}s = \epsilon(v_1 + \rho_1) + O(\epsilon^2) \tag{2.15}$$

and

$$-2\epsilon g(\alpha) = v - \int^{\rho} \frac{a(s)}{1+s}\mathrm{d}s = \epsilon(v_1 - \rho_1) + O(\epsilon^2), \tag{2.16}$$

where $\epsilon f(\beta)$ and $\epsilon g(\alpha)$ are the Riemann invariants for the problem, to be determined from the boundary conditions (2.4) and (2.5).

The slope conditions (2.10) are then approximated by

$$\pm\frac{\mathrm{d}x}{\mathrm{d}t} = 1 + \epsilon^2(\bar{\Gamma}\rho_1 + \tfrac{1}{2}A\rho_1^2) = 1 + \epsilon^2 C, \tag{2.17}$$

where $\Gamma = \epsilon\bar{\Gamma}, \bar{\Gamma} = O(1)$ and $\rho_1 \cong f(\beta) + g(\alpha)$.

Discontinuities when they form in the flow field are subject to the jump conditions (2.3). We require for right-running shocks a Lagrangian shock speed given by

$$u = 1 + \epsilon u_1 + \epsilon^2 u_2 + O(\epsilon^3) \tag{2.18}$$

and an expansion for $p(\rho)$ determined from (2.8), namely

$$p = \rho + (\Gamma - 1)\rho^2 + \tfrac{1}{3}(A+3)\rho^3 + O(\epsilon^4), \tag{2.19}$$

where ρ is given by (2.12). We have corresponding to (2.3) then the jump conditions

$$O(\epsilon) : [v_1 - \rho_1] = 0, \tag{2.20}$$

$$O(\epsilon^2) : u_1[v_1] = 0, \tag{2.21}$$

$$O(\epsilon^3) : 2u_2[\rho_1] = \bar{\Gamma}[\rho_1^2] + \tfrac{1}{3}A[\rho_1^3]\ . \tag{2.22}$$

From (2.16) and (2.20) we see that the left-running Riemann invariant $g(\alpha)$ is continuous across right-running shock waves. Equation (2.21) requires that $u_1 \equiv 0$ and from (2.18) and (2.22) u can be written as

$$u \sim 1 + \epsilon^2 u_2 = 1 + \epsilon^2\frac{\bar{\Gamma}}{2}\frac{[\rho_1^2]}{[\rho_1]} + \epsilon^2\frac{A}{6}\frac{[\rho_1^3]}{[\rho_1]}\ , \quad \rho_1 = f(\beta) + g(\alpha). \tag{2.23}$$

In the case of a left-running shock , the shock speed is $-u$.

The problem is now the integration of (2.17) giving characteristic curves along which the Riemann invariants ϵf and ϵg propagate, where f and g are determined from imposing boundary conditions (2.4) and (2.5). The motion of any discontinuity in the flow field is calculated using (2.23). The conditions under which realistic shock

discontinuities can be inserted is more complicated than for classical weak shock theories. We simply summarize the results obtained by Cramer & Kluwick (1984) for the case of unidirectional waves with the obvious extension made here to two-wave families.

When $\Lambda > 0$ an existing discontinuity must satisfy the speed ordering condition

$$\left.\frac{\mathrm{d}x}{\mathrm{d}t}\right|_a > u \geqslant \left.\frac{\mathrm{d}x}{\mathrm{d}t}\right|_b, \tag{2.24}$$

where $\mathrm{d}x/\mathrm{d}t|_a$ and $\mathrm{d}x/\mathrm{d}t|_b$ are evaluated for $\rho_1 = \rho_{1_a}$ and $\rho_1 = \rho_{1_b}$ and the subscripts a and b refer to conditions before and after a shock.

When $\Lambda < 0$ the speed ordering condition is

$$\left.\frac{\mathrm{d}x}{\mathrm{d}t}\right|_a \geqslant u > \left.\frac{\mathrm{d}x}{\mathrm{d}t}\right|_b. \tag{2.25}$$

Equations (2.24), (2.25) are presented here as admissibility conditions for shock propagation. It must be recognized that in recent years the question of shock admissibility for materials with non-convex equations of state has been the subject of extensive study both from an applied and a theoretical perspective. That non-convexity arises here can readily be seen on writing Γ in the form

$$\Gamma = \left.\frac{v^3}{2a^2}\frac{\partial^2 p}{\partial v^2}\right|_s. \tag{2.26}$$

When $\Gamma_0 = O(\epsilon)$ and $\Lambda = O(1)$ the wave speed ordering condition given by (2.24), (2.25) is necessary and sufficient to exclude inadmissible shocks. This is not always the case. A more general admissibility criterion was developed in Liu (1976*a*,*b*) in terms of an entropy condition which ensures the existence of a viscous shock layer structure. This entropy condition can be stated in terms of the Rayleigh line connecting two thermodynamic states lying entirely above (compressive shock) or entirely below (expansion shock) the shock adiabat. In Cramer & Crickenberger (1991) this criterion is used in a description of shocks in dense gases, and in Kluwick (1993), Kluwick & Scheichl (1996) in the problem of transonic nozzle flow in dense gases. These results for dense gases assume that now $\Gamma = O(\epsilon^2)$ and $\Lambda = O(\epsilon)$ and a wave description involves a third nonlinear parameter proportional to $\partial^2\Gamma/\partial\rho^2$. The analysis of this present paper could forseeably be extended to a consideration of this case.

The permissible *equalities* in (2.24), (2.25) represent sonic shocks in the gas flow, a possibility excluded from classical weak shock theory. It is possible to interpret (2.24), (2.25) in terms of permissible density jumps. Following Cramer & Kluwick (1984) it is first more convenient to scale

$$\hat{\rho}_1 = \frac{\Lambda}{\Gamma}\rho_1 = \frac{\Lambda}{\Gamma}(f(\beta) + g(\alpha)) = F(\beta) + G(\alpha). \tag{2.27}$$

For $\Lambda > 0$, permissible jumps are when $\hat{\rho}_{1_a}$ and $\hat{\rho}_{1_b}$ lie between the lines $\hat{\rho}_{1_b} = \hat{\rho}_{1_a}$ and $\hat{\rho}_{1_b} = -\frac{1}{2}(\hat{\rho}_{1_a} + 3)$. For $\Lambda < 0$, $\hat{\rho}_{1_a}$ and $\hat{\rho}_b$ must lie between the lines $\hat{\rho}_{1_b} = \hat{\rho}_{1_a}$ and $\hat{\rho}_{1_b} = -(2\hat{\rho}_{1_a} + 3)$. This can be contrasted with a classical gas where jump strength is not restricted, only the sign of the jump must satisfy $\Gamma[\rho_1] > 0$. An obvious conclusion is that if an imposed discontinuity in the gas flow exceeds a critical strength (corresponding to sonic conditions) then the discontinuity will disintegrate into a sonic shock and wave fan combination. A similar analysis can be applied to

an imposed wave fan discontinuity. The wave fan will be instantaneously unstable if density values in the wave fan lie in both

$$\hat{\rho}_1 > -1 \tag{2.28}$$

and

$$\hat{\rho}_1 < -1 \tag{2.29}$$

regions and a shock–fan combination will form. This is interpreted as a limitation on the strength of the wave fan.

We now proceed to integrate (2.17) using expansions (2.11)–(2.14). If α and β are parameterized by the condition that $\alpha = \beta = \omega t$ on $x = 0$ then (2.17) implies that to $O(\epsilon^3)$

$$\omega(x-t) = -\beta + \epsilon^2\frac{\bar{\Gamma}}{2}f(\beta)(\alpha-\beta) + \epsilon^2\frac{\bar{\Gamma}}{2}\int_\beta^\alpha g(s)\mathrm{d}s + \epsilon^2\frac{\Lambda}{4}f^2(\beta)(\alpha-\beta) + \epsilon^2\frac{\Lambda}{2}f(\beta)\int_\beta^\alpha g(s)\mathrm{d}s + \epsilon^2\frac{\Lambda}{4}\int_\beta^\alpha g^2(s)\mathrm{d}s \tag{2.30}$$

and

$$\omega(x+t) = \alpha + \epsilon^2\frac{\bar{\Gamma}}{2}g(\alpha)(\alpha-\beta) + \epsilon^2\frac{\bar{\Gamma}}{2}\int_\beta^\alpha f(s)\mathrm{d}s + \epsilon^2\frac{\Lambda}{4}g^2(\alpha)(\alpha-\beta) + \epsilon^2\frac{\Lambda}{2}g(\alpha)\int_\beta^\alpha f(s)\mathrm{d}s + \epsilon^2\frac{\Lambda}{4}\int_\beta^\alpha f^2(s)\mathrm{d}s. \tag{2.31}$$

The evolution of f and g on the closed boundary $x = 0$ is described by a nonlinear functional equation – a mapping of the time taken for a wavelet leaving $x = 0$ to return to the boundary with the associated change in the signal carried by the wavelet.

Consider a wave which leaves $x = 0$ at $t = \alpha/\omega$ and returns to $x = 0$ at time $t = \beta/\omega$, having made a complete traversal of the pipe. We assume the wave leaves with the signal value $f(\beta) = g(\beta)$ and arrives back with $g(\alpha)$; then using (2.30), (2.31) we have

$$\alpha = \beta + 2\omega - \epsilon^2\frac{\bar{\Gamma}}{2}\{g(\beta)+g(\alpha)\}(\alpha-\beta) - \epsilon^2\bar{\Gamma}\int_\beta^\alpha g(s)\mathrm{d}s - \epsilon^2\frac{\Lambda}{2}\int_\beta^\alpha g^2(s)\mathrm{d}s - \epsilon^2\frac{\Lambda}{2}\{g(\alpha)\int_\beta^\alpha g(s)\mathrm{d}s + g(\beta)\int_\beta^\alpha g(s)\mathrm{d}s\} - \epsilon^2\frac{\Lambda}{4}\{g^2(\alpha)+g^2(\beta)\}(\alpha-\beta). \tag{2.32}$$

The variation in the Riemann invariant ϵg after the wave makes one complete traverse of the tube is given by

$$\epsilon g(\alpha) - \epsilon g(\beta) = -\mu\omega h'(\omega t_1)\,, \quad t_1 = \frac{\beta}{\omega} + 1 + O(\epsilon^2) \tag{2.33}$$

on using (2.15), (2.16) and the boundary conditions (2.4), (2.5), where t_1 is the arrival time of the wave at the boundary $x = 1$. It should be emphasized that equations (2.32) and (2.33) describe the *evolution* of the wave form on the boundary $x = 0$: at this stage no periodicity condition is imposed. With zero values for g given on an initial interval then the evolution from an undisturbed state to a final periodic state could be examined along similar lines to Seymour & Mortell (1985). The initial

behaviour of the signal would be represented by the linear functional equation

$$\left.\begin{aligned} g(\alpha) &= g(\beta) - \omega h'(\beta + \omega), \\ \alpha &= \beta + 2w, \end{aligned}\right\} \tag{2.34}$$

with the Mach number of the gas $\epsilon = \mu$. Equation (2.34), describing the initial growth of the signal, has no bounded solutions with unit period when $\omega = \omega_m = \frac{1}{2}m$ $(m = 1, 2, 3\ldots)$. These are the linear resonant frequencies. In this paper we are interested in bounded periodic solutions with unit period for operating frequencies in the neighbourhood of ω_m given by

$$\omega = \omega_m(1 + \epsilon^2 \Delta), \qquad \Delta = O(1). \tag{2.35}$$

The frequency detuning is $O(\epsilon^2\omega)$, chosen to appear in (2.32) at the same order as the nonlinearity.

After a long time the signal settles down to a periodic state and the difference $g(\alpha) - g(\beta)$ in (2.33) is, from (2.32), $O(\epsilon^2\omega)$. This gives a Mach number for the long time behaviour of $\epsilon = \mu^{1/3}$, representing a growth in the signal from $O(\mu)$ initially to $O(\mu^{1/3})$ finally.

Similar to the perfect gas case this estimate can be derived directly from an energy balance assuming that the steady-state periodic solution contains shock discontinuities. The energy dissipated by a shock per unit time $\rho_0 T_0 a_0 [s]$ then has to be supplied by the work of the piston per unit time $\rho_0 a_0^3 pv$. Owing to the assumption $\Gamma = O(\epsilon)$ adopted here, $[s]|_{c_{v_0}} = O(\epsilon^4)$ which together with $p = O(\epsilon))$ and $v = O(\mu)$ immediately yields $\epsilon = O(\mu^{1/3})$ as before. In passing note that this order of magnitude relationship holding for resonant dense gas oscillations in closed tubes is of the same form as the corresponding result for resonating perfect gas oscillations in open tubes (Jimenez 1973). Consequently, the power required to drive the piston is of comparable magnitude in both cases.

We can simplify (2.32) and (2.33) by retaining only terms to $O(\epsilon^2\omega)$ with the approximation $\alpha - \beta \simeq 2\omega$ in the ϵ^2 terms of (2.32). Further, the fact that u and p have zero mean over one cycle means that

$$\int_{\phi}^{\phi+m} f(s)\mathrm{d}s = \int_{\phi}^{\phi+m} g(s)\mathrm{d}s = 0\,. \tag{2.36}$$

The functional equation (2.32), (2.33) then reduces to

$$g(\alpha) = g(\beta) - \epsilon^2 w h'(\beta + \tfrac{1}{2}m), \tag{2.37}$$

$$\alpha = \beta + m + \epsilon^2 m\delta - \epsilon^2 m\bar{\Gamma}\, g(\beta) - \epsilon^2 \frac{m\Delta}{2} g^2(\beta)\,, \quad m = 1, 2, 3\ldots \tag{2.38}$$

where

$$\delta = \Delta - \frac{\Delta}{2}\int_{\phi}^{\phi+m} g^2(s)\mathrm{d}s\,. \tag{2.39}$$

The integral term in (2.39) represents a shift in the linear resonant frequency due to the local interaction of oppositely travelling waves. Wave interaction increases $(\Delta < 0)$ or decreases $(\Delta > 0)$ the travel time of the wavelets and consequently alters the resonant frequency.

Equations (2.37)–(2.39) represent the basic functional equation for resonant oscillations in a closed tube. We can note two special cases. If $|\Delta g(\beta)|$ is negligible compared to $\bar{\Gamma}$ then (2.38) is equivalent to the case where $\bar{\Gamma}$ is an order-one constant. In par-

ticular for an ideal gas where $\Gamma = \frac{1}{2}(\gamma + 1)$, and γ is the ratio of specific heats, we reproduce the functional equation analysed extensively in Seymour & Mortell (1980) and Mortell & Seymour (1979). In the second case $\bar{\Gamma} = 0$, the undisturbed state is on the transition line and equations (2.37),(2.38) are *mathematically* similar to the functional equation derived by Seymour & Mortell (1973*b*) for resonant oscillations in an open tube.

3. Small-rate approximation: periodic response

The derivation of the functional equations (2.37)–(2.39) makes no assumption regarding the acceleration rate of the evolving signal: as such it represents a small-amplitude ($\epsilon \ll 1$), finite-rate evolution equation for the signal. A long-time-periodic response is derived by an expansion in the small rate limit $|\epsilon^2 m \mathrm{d}g/\mathrm{d}s| \ll 1$. Equation (2.38) then implies that

$$g(\alpha) = g(\beta) + \epsilon^2 m(\delta - \bar{\Gamma} g(\beta) - \tfrac{1}{2} m \Lambda g^2(\beta)) g'(\alpha)[1 + O(\epsilon^2 m g')] \tag{3.1}$$

and then equation (2.37) can be approximated by the ordinary differential equation

$$(\bar{\Gamma} g(s) + \tfrac{1}{2}\Lambda g^2(s) - \delta)\frac{\mathrm{d}g}{\mathrm{d}s}(s) = \frac{1}{2}\frac{\mathrm{d}h}{\mathrm{d}s}(s + m/2), \quad \delta = \Delta - \frac{\Lambda}{2}\int_s^{s+m} g^2(r)\mathrm{d}r. \tag{3.2}$$

Periodic solutions, $g(s+m) = g(s)$, of (3.2) are sought which satisfy the mean condition

$$\int_s^{s+m} g(r)\mathrm{d}r = 0. \tag{3.3}$$

Solutions of equation (3.2),(3.3) describe the periodic signal on the closed boundary $x = 0$. In the analysis that follows we consider specifically the resonance $m = 1$ and the applied forcing frequency $h(s) = \frac{1}{3}\sin(2\pi s)$.

Again we note two special cases of (3.2),(3.3). When $\bar{\Gamma} \neq 0, \Lambda = 0$ then (3.2) describes steady-state resonant oscillations in a closed tube for an ideal gas. The results of Chester (1964) indicate the existence of a resonance frequency band where shock waves occur in the flow and outside which the wave profile is continuous. The second case occurs when $\bar{\Gamma} = 0, \Lambda \neq 0$ and arises in the context of ideal gas oscillations in an open tube, see Jimenez (1973), Seymour & Mortell (1973*b*), Chester (1981), Chester & Moser (1982). In contrast to the closed tube case, narrow compression and expansion regions occur in the signal. In Chester (1981) and Chester & Moser (1982) the influence of dissipation on the signal is also investigated.

In the analysis that follows we distinguish between integral curves of (3.2) (now with $m = 1, h = \frac{1}{3}\sin(2\pi s)$) and the physical signal which must satisfy an additional mean constraint. The integral curves of (3.2) satisfy

$$3\bar{\Gamma} g^2 + \bar{\Lambda} g^3 + \sin(2\pi s) - 6\delta g = Q, \qquad s \in [\phi, \phi + 1], \tag{3.4}$$

where Q is a constant. Clearly an integral curve which is periodic and satisfies the mean condition (3.3), with $m = 1$, can represent the physical signal. When no such curve exists a signal can still be constructed composed of disjoint integral curves – the signal will include discontinuities. To determine the strength and position of these discontinuities we impose the condition that they propagate as periodic shocks in the flow. From equation (2.23) we see that shock discontinuities propagate with speeds $\pm u$. Integration of (2.23) is possible assuming that there is negligible distortion of the signal in the periodic state. If we consider a shock of constant strength $[\rho_1] = [g]$

as measured on the boundary $x = 1$ then this shock will return to the boundary after a time T given (on integrating equation (2.23)) by

$$T = 2 - \frac{\epsilon^2}{\omega}\int_0^1 u_2(\beta)\mathrm{d}\beta + o\left(\epsilon^2\right). \tag{3.5}$$

Periodicity requires that $T = 1/\omega$ and hence that the average perturbed shock speed is

$$\tilde{u}_2 := \int_0^1 u_2(\beta)\mathrm{d}\beta = \Lambda. \tag{3.6}$$

This in turn implies, from (2.23), that a shock discontinuity $[g]$ satisfies

$$3\bar{\Gamma}[g^2] + \Lambda[g^3] - 6\delta[g] = 0, \qquad \delta = \Lambda - \frac{\Lambda}{2}\int_\phi^{\phi+1} g^2(s)\mathrm{d}s. \tag{3.7}$$

In other words physical discontinuities can only be constructed from integral curves that have the same Q values. In addition we require that the discontinuous signal can be imbedded in the evolution equations (2.37),(2.38) as a stable periodic flow. For a stable imbedding of a periodic discontinuity located at characteristic $\beta = \beta_s$ on $x = 0$ the travel times of wavelets $f_b = \lim_{h\to 0} f(\beta_s - h)$ and $f_a = \lim_{h\to 0} f(\beta_s + h)$ denoted by T_b and T_a must satisfy the inequality

$$T_b > \frac{1}{\omega} > T_a. \tag{3.8}$$

Using (2.38) we then have the inequality

$$\bar{\Gamma} g_a + \frac{\Lambda}{2}g_a^2 + \frac{\Lambda}{2}\int_\phi^{\phi+1} f^2(s)\mathrm{d}s > \Lambda > \bar{\Gamma} g_b + \frac{\Lambda}{2}g_b^2 + \frac{\Lambda}{2}\int_\phi^{\phi+1} f^2(s)\mathrm{d}s \tag{3.9}$$

which can be written in the form

$$\tilde{C}_a > \tilde{u}_2 > \tilde{C}_b \tag{3.10}$$

where $\tilde{C}_{a,b}$ is the average perturbed characteristic speed

$$\tilde{C}_{a,b} := \int_\phi^{\phi+1} C_{a,b}(s)\mathrm{d}s \tag{3.11}$$

with $C_{a,b}$ given by equation (2.17). This is clearly the requirement that the average shock speed lies between the the average wave speeds for the signal entering the shock. The possibility of sonic shocks for equation (3.2), representing average sonic conditions for the propagating signal through one traversal of the wavetube will introduce equalities into (3.10). From our discussion in §2 we deduce that if $\Lambda > 0$ the average speed ordering condition is now

$$\tilde{C}_a > \tilde{u} \geqslant \tilde{C}_b, \tag{3.12}$$

i.e. $T_b \geqslant 1 > T_a$, whereas if $\Lambda < 0$ then

$$\tilde{C}_a \geqslant \tilde{u} > \tilde{C}_b \tag{3.13}$$

i.e. $T_b > 1 \geqslant T_a$.

It is possible for discontinuities in (3.2) to satisfy the average speed ordering conditions (3.12),(3.13) and yet violate the local ordering conditions (2.24),(2.25). Again this is usefully interpreted in terms of permissible discontinuities. We illustrate

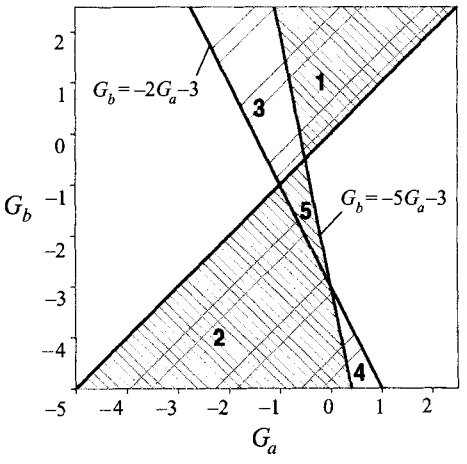

FIGURE 1. Shock jump discontinuities for $\Lambda < 0$.

this for the case $\Lambda < 0$. On the boundary $x = 0$, $\hat{\rho}_1$ is given by the representation (2.27) with $F(\beta) = G(\alpha)$. For a discontinuity to be locally stable there is the requirement that the functions $G_a = (\Lambda/\bar{\Gamma})g_a$ and $G_b = (\Lambda/\bar{\Gamma})g_b$ must lie between the lines $G_a = G_b$ and $G_b = -5G_a - 3$. In contrast a stable periodic discontinuity of (3.2) must lie between $G_a = G_b$ and $G_b = -2G_a - 3$. These regions are shown in figure 1. The shaded regions represent discontinuities described by G_a, G_b. Regions 1, 2, 5 represent permissible shock jump discontinuities satisfying (2.25). Regions 1–4 combine to represent admissible discontinuities for (3.2). We highlight the fact that when $G_b > -1/2$ or $G_b < -3$ then region 3 or 4 will represent discontinuities of (3.2) allowed by (3.13) but which are actually physically unstable discontinuities violating (2.25). An imposed discontinuity of this strength on the boundary would instantaneously disintegrate to form a sonic shock and wave fan combination propagating into the interior of the tube. That a discontinuity of this strength is predicted for equation (3.2) is due to the effect of refocusing of the wave fan as it goes through one traversal of the tube.

Equation (3.2) with $\bar{\Gamma} = 0$ has been derived in the different, though related, problem of a classical resonating gas in an open tube and it is important to highlight the differences between the two problems for this particular limiting case. These differences relate particularly to the inclusion of shock discontinuities which is a central concern of this paper. In the classical open tube problem no shock theory can be used to generate a shock condition equivalent to equation (3.10). This point is clearly made in Jimenez (1973). The assumption of isentropic flow for the equations of motion when used to $O(\epsilon^3)$ is inconsistent with shocks which produce an entropy jump also at this same order. As a consequence discontinuities in the classical open tube problem must be understood in terms of refocused wave fans – the refocusing due to the imposed open boundary condition. This inconsistency does not arise for BZT-fluids as the entropy jump across the shock occurs at a higher order. Discontinuities when they occur represent genuine shock behaviour for which a shock theory has been developed. A more general model equation for the open tube problem which includes dissipation is used in Chester (1981) not only to provide a structure to the expansive discontinuities of (3.2) but more importantly to actually locate their positions. In the present context of dense gases in closed tubes a shock theory has been used to locate the discontinuities of (3.2). This theory leads to condition (3.10) for the shock speeds.

The inclusion of dissipative effects in the form of thermoviscous diffusivity provides a structure then to the already determined shock discontinuities as we now show.

4. Dissipative effects

Thermoviscous effects can readily be included in our analysis through a straightforward application of multiple scaling (see Cramer & Kluwick 1984 for an application to unidirectional motion). The signal *on the boundary* $x = 0$ is given by the long-time evolution equation

$$\frac{\partial g}{\partial \tau} + \left(\bar{\Gamma} g + \frac{\Lambda}{2} g^2 - \Delta + \frac{\Lambda}{2}\int_t^{t+1} g^2(r)\mathrm{d}r\right)\frac{\partial g}{\partial t} + \frac{\pi}{3}\cos(2\pi t) = \nu\frac{\partial^2 g}{\partial t^2}, \tag{4.1}$$

where

$$g(t+1) = g(t). \tag{4.2}$$

The signal evolves on the long timescale $\tau = \epsilon^2 t$ but is periodic in the fast scale $t = s$. Equations (4.1),(4.2) constitute a *small-amplitude, small-rate* approximation. The coefficient ν represents an effective acoustic diffusivity given by

$$\nu = \frac{1}{2\epsilon^2 Re}\left(\frac{\lambda_0}{\mu_0} + 2 + \frac{\beta_0^2 T_0 a_0^2}{C_{p_0} Pr}\right) \tag{4.3}$$

where λ_0 and μ_0 denote first and second viscosities, T_0 temperature, Pr the Prandtl number and β_0 the coefficient of thermal expansion, all evaluated in the mean reference state. In the inviscid limit $\nu \to 0$ equation (4.1) could also be constructed as a two-variable expansion of the functional equation (2.37),(2.38).

The steady-state limit of (4.1) is given by

$$\left(\bar{\Gamma} g + \frac{\Lambda}{2} g^2 - \Delta + \frac{\Lambda}{2}\int_t^{t+1} g^2(r)\mathrm{d}r\right)\frac{\mathrm{d}g}{\mathrm{d}t} + \frac{\pi}{3}\cos(2\pi t) = \nu\frac{\mathrm{d}^2 g}{\mathrm{d}t^2}, \tag{4.4}$$

where we look for periodic solutions satisfying a zero mean condition.

To simplify the subsequent analysis we introduce the transformation

$$G = \frac{\Lambda}{\bar{\Gamma}} g, \qquad y = \frac{|\Lambda|}{\Lambda} t \tag{4.5}$$

following Cramer & Kluwick (1984). On substituting (4.5) into (4.4) we have the ordinary differential equation

$$(\tfrac{1}{2}G^2 + G - \lambda)\frac{\mathrm{d}G}{\mathrm{d}y} + A\cos(2\pi y) = \bar{\nu}\frac{\mathrm{d}^2 G}{\mathrm{d}y^2}, \tag{4.6}$$

where

$$\lambda = \frac{\Lambda}{\bar{\Gamma}^2}\Delta - \frac{1}{2}\int_y^{y+1} G^2(r)\mathrm{d}r, \tag{4.7}$$

$$A = \frac{\pi \Lambda^3}{3\bar{\Gamma}^3|\Lambda|} \tag{4.8}$$

and

$$\bar{\nu} = \frac{\nu|\Lambda|}{\bar{\Gamma}^2}. \tag{4.9}$$

Again we look for periodic solutions of (4.4) satisfying a zero mean condition.

The variables $\lambda, A, \bar{\nu}$ can be used to identify a family of similar solutions. From our discussion of shock discontinuities we need the additional mild constraint that similar flows will have the same sign of A.

From (4.8) we see that the parameter A describes the dependence of the solution on the ratio of the nonlinear parameters A/Γ and so is determined by the thermodynamic state of the undisturbed fluid. In the limit as $A \to \infty$ solutions of (4.1) are obtained with $\Gamma = 0$. The classical gas solution arises in the limit $A \to 0$. The parameter λ gives an effective detuning parameter and includes the influence of wave interaction.

Numerical solutions of (4.6) are presented in §5. At this point we give, for completeness, an analysis of the weak shock structure which is identical to that given in Cramer & Kluwick (1984).

We introduce the variables

$$R = \frac{2}{[G]}\left(G - \frac{G_a + G_b}{2}\right), \qquad \bar{t} = [G]^2 \frac{t - t_0}{24\bar{\nu}} \tag{4.10}$$

and choose $R(t_0) = \frac{1}{2}(G_a + G_b)$ where t_o is the location of the jump discontinuity as given by inviscid theory. On assuming that within the shock the applied forcing is constant we can show that R satisfies the differential equation (5.4) in Cramer & Kluwick (1984) and has the profile given by

$$\bar{t} = \frac{1}{B^2 - 1}\left(2\ln\left(\frac{R}{B} + 1\right) + B\ln\left(\frac{1 - R}{1 + R}\right) - \ln(1 - R^2)\right), \qquad B > 1 \tag{4.11}$$

or

$$\bar{t} = \frac{1}{2}\ln\left(\frac{1 - R}{1 + R}\right) - \frac{R}{1 + R}, \qquad B = 1, \tag{4.12}$$

where $B = (6/[G])\left(1 + (\frac{1}{2}(G_a + G_b))\right)$. The case $B = 1$ corresponds to sonic conditions and it is seen from (4.12) that the shock structure is algebraic rather than exponential in character. Within the context of resonant oscillations in open tubes similar observations have been made, see Chester (1981).

5. Analytic and numerical results

In the limit $\bar{\nu} \to 0$ equation (4.6) models steady-state inviscid flow. In this limit we analyse the integral curves of (4.6) to constuct a steady-state signal. We require that G is single valued and satisfies a zero mean condition. Equation (4.6) has singular points at $y = 1/4, 3/4$ with values of G satisfying

$$\tfrac{1}{2}G^2 + G - \lambda = 0. \tag{5.1}$$

It is clear from (5.1) that for $\lambda < -1/2$ there are no singular points and that from (4.6) the corresponding integral curves have bounded derivatives. In this case all integral curves are periodic and there exists a unique curve which satisfies the zero mean condition and represents a physical signal. For $\lambda > -1/2$ saddle singularities occur at the points $(1/4+n, -1+(1+2\lambda)^{1/2}), (3/4+n, -1-(1+2\lambda)^{1/2})$, and centres are located at $(1/4+n, -1-(1+2\lambda)^{1/2}), (3/4+n, -1+(1+2\lambda)^{1/2})$ where $n = 0, \pm 1, \pm 2, \cdots$.

The role of the integral curves emanating from the saddle singularities in constructing discontinuous solutions can be understood in terms of the critical points of the functional mapping (2.37),(2.38). Saddle singularities of (4.6), with $\bar{\nu} = 0$, represent wavelets in the signal which complete one cycle of the tube in a period of the piston. When the steady-state solution includes these saddle points then the

long-time behaviour can be described in terms of an initial signal emanating from a vanishingly small neighbourhood of these fixed points. This is the case in figures 2(*a*) and 2(*b*) where inviscid solutions are constructed from the integral curves of (4.6). The discontinuities inserted satisfy the speed ordering conditions (3.13) and the discontinuous solution has zero mean. Figures 2(*a*)–2(*d*) give representative solutions for various values of the similarity variables A and λ. The qualitative differences exhibited correspond to identifiable regions in the (A, λ) parameter space as indicated in figure 3. A resonant band is indicated in figure 3 including the regions 1–4 in which the solutions involve shock discontinuities. For a particular fluid the parameter A is determined from (4.8). Then both the frequency width of the resonant shock band and the qualitative features of the solution as the effective frequency λ is varied can readily be identified.

For small values of A we expect the solutions to exhibit similar qualitative features to a classical gas. This is confirmed in figure 2(*a*) where the solution is constructed from separatrices that connect the saddle points. Figure 2(*a*) gives the structure of the signal for values of A and λ in region 1 in figure 3. All results are for $A < 0$. For purposes of discussion we will refer to discontinuities which decrease with y as compression shocks and discontinuities which increase with y as expansion shocks. There is a single compression discontinuity inserted into the separatrices of the saddle points. Figure 2(*b*) describes solutions in region 2 of figure 3. This region is distinguishable from region 1 by a qualitative change in the integral curves of (4.6). However shock solutions can still be constructed from saddle point integral curves and the solution profiles are similar to those in figure 2(*a*). Regions 1 and 2 of figure 3 then represent parameter regimes where the signal supports a single compressive discontinuity. If we hold λ fixed and increase A the compressive discontinuity becomes sonic on the boundary with region 3. An expansion shock then forms and the signal within region 3 is characterized by two shocks one of which (the compression shock) is sonic ($T_a = 1$). A representative signal is plotted in figure 2(*c*). If we continue to increase A holding λ fixed the solution enters the parameter region 4 of figure 3. The expansion shock now also becomes sonic as seen from figure 2(*d*). Critical points of (4.6) are not involved in construction of the solution. The solutions in this parameter region qualitatively resemble those discussed in Chester (1981) for a classical gas in an open tube.

We have discussed essentially how the signal responds to increasing values of the parameter A for fixed λ. We now investigate how the signal structure varies with λ when A is held fixed. In figure 4(*a*) we plot the wave amplitude of the signal as a function of λ for $A = 1$. This response curve is comparable to response curves for a classical resonating gas, see for example Seymour & Mortell (1973*a*). In figure 4(*b*) we plot the imposed driving frequency (actually the scaled frequency $A\Delta/\Gamma^2$) against the effective frequency λ. The effect of the interaction term in (4.7) is primarily seen in a shift of the resonance peaks in figure 4(*a*). As one might expect the solution profiles are similar to the classical gas and this is borne out in figure 5 where the solution profile is plotted for a range of λ. As λ decreases from $\lambda = 0.6$ to $\lambda = -0.6$ the initially continuous solution enters regions 1 and 2 of figure 3 where a single compressive discontinuity is formed. On detuning through the resonant band, the shock discontinuity moves relative to the phase of the piston until eventually a continuous integral curve satisfies the mean condition. For frequencies away from resonance the continuous signal is well approximated by a linear theory. Care must be taken in the interpretation of these profiles. For values of $\lambda < 0.11903$ (the frequency $\lambda = 0.11903$ is labelled in figure 4*a* with an open circle) the solution discontinuity

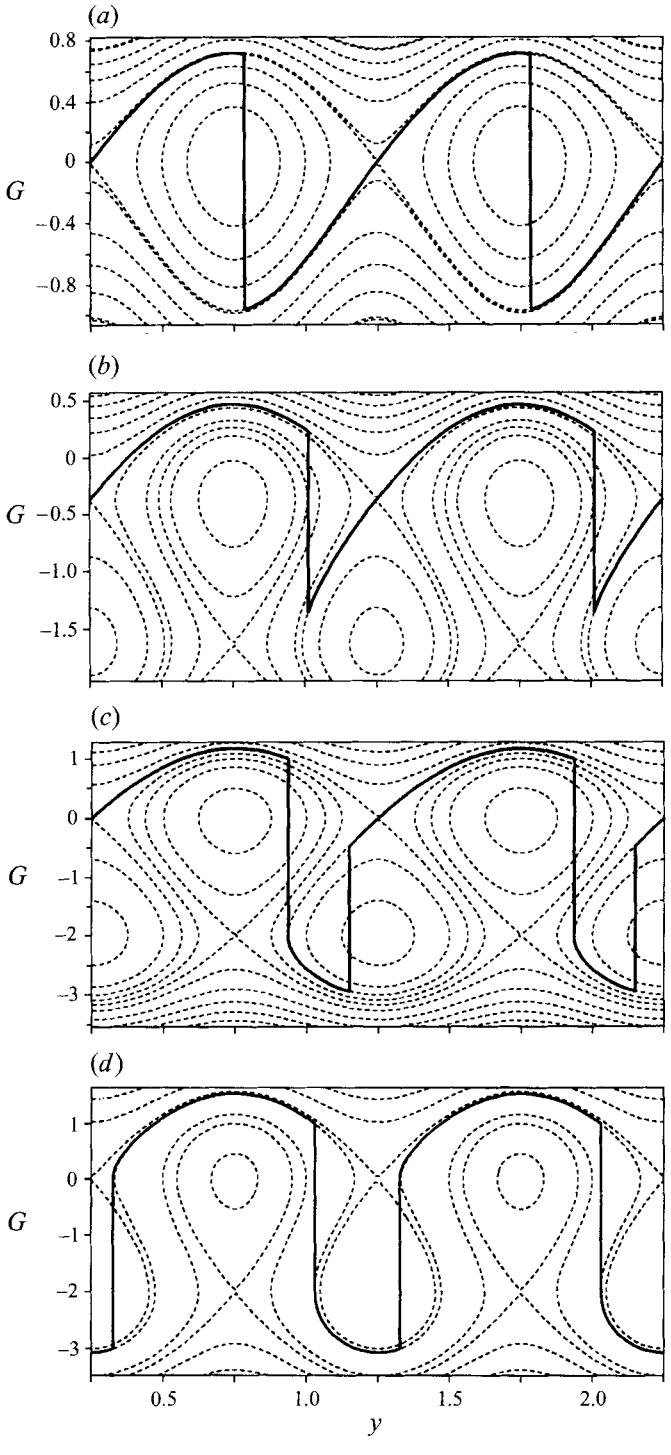

FIGURE 2. Signal for A, λ values in the regions shown in figure 3 (*a*) region 1, (*b*) region 2, (*c*) region 3, (*d*) region 4.

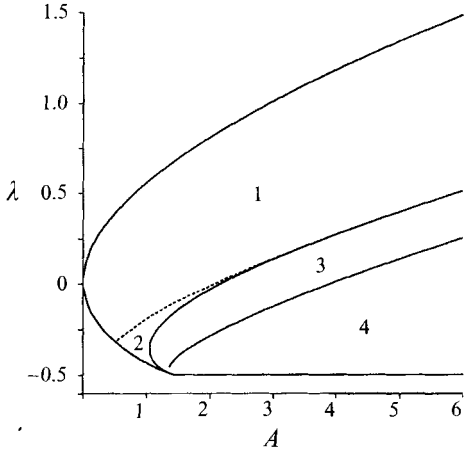

FIGURE 3. Resonant shock band.

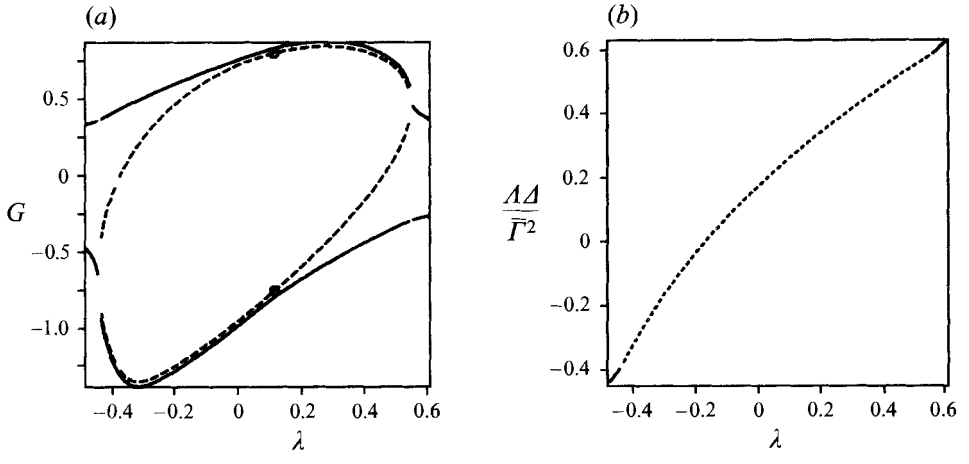

FIGURE 4. (*a*) Signal amplitudes for $A = 1$. Maximum and minimum amplitudes (——), shock amplitudes (– – –). (*b*) Variation of $\Lambda\Delta/\bar{\Gamma}^2$ with λ for $A = 1.0$.

violates the local speed ordering conditions, namely (2.25), and the discontinuity lies in region 3 of figure 1. For these frequencies the discontinuities should be interpreted as sonic shock/fan regions of rapid transition.

As A increases the situation becomes more complicated. In figures 6–8 the results are given for $A = 5$. A transition from one shock to two shocks as λ decreases through the resonant frequency band is shown in figure 7. This coresponds to a transition through regions 1, 3 and 4 of figure 3 . The transition occurs through the single compressive shock becoming sonic at a point on the boundary between regions 1 and 3. The expansion shock formed as λ continues to decrease in turn becomes sonic on entering region 4. The strength of the two shocks decay as λ is further detuned away from resonance. Eventually at $\lambda = -0.5$ a continuous profile can be constructed. The resonant response diagram is given by figure 6(*a*) where the shock amplitudes are indicated. Again in interpreting the discontinuities constructed we note that the compression shock lies outside the local shock inequalities given by (2.25) for $\lambda < 0.7478$ – this frequency is marked by a closed circle in figure 6(*a*). The expansion shock also violates (2.25) for $-0.0022 < \lambda < 0.158$ – a frequency interval

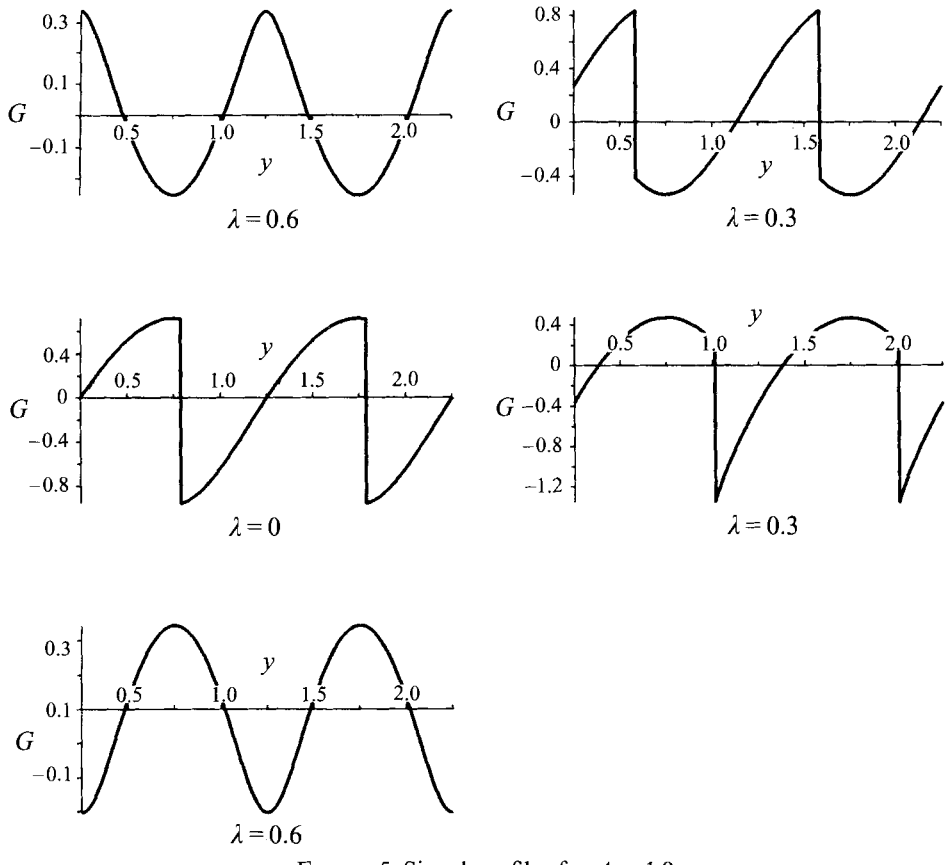

FIGURE 5. Signal profiles for $A = 1.0$.

marked by open circles. For frequencies where (2.25) is violated the discontinuity models what is locally a sonic shock/fan transition. The relationship between the effective frequency and the actual forcing frequency is indicated in figure 6(*b*). The dotted curves relate to solutions found in the shock regions 1, 3 and 4 of figure 3. In contrast to figure 4(*b*) ($A = 1$) there exist *multiple solutions* with different λ values for a given Δ. In particular an acceptable continuous solution branch exists to replace solutions in region 3 of figure 3. To investigate this further we solve equation (4.6) to determine the viscous profiles for $\bar{\nu} = 0.02$. Periodic solutions satisfying a zero mean were constructed using a variable-order, variable-step size, finite difference algorithm. For each λ the solution was constructed using a continuation algorithm from an initial approximation given by linear theory for λ large and positive. This could alternatively be interpreted as a *slow passage through resonance* formulation. These viscous results are superimposed on the inviscid curves of figure 6(*b*) as indicated and in figures 8(*a*) and 8(*b*) we compare viscous and inviscid profiles for $A = 5$, and $\bar{\nu} = 0.02$. In figure 8(*a*) ($\lambda = 0.75$) we have essentially a classical shock structure with slight deviation from a Taylor profile. In figure 8(*b*) ($\lambda = -0.25$) both shocks are sonic and the algebraic behaviour of the shock structure is evident as predicted by equation (4.12). There is an obvious phase shift in the viscous structure from the inviscid position.

We conclude with an examination of the limiting case $\bar{\Gamma} = 0, \Delta \neq 0$. The transformations (4.5) are singular under this limit and so we revert to equation (3.2) with

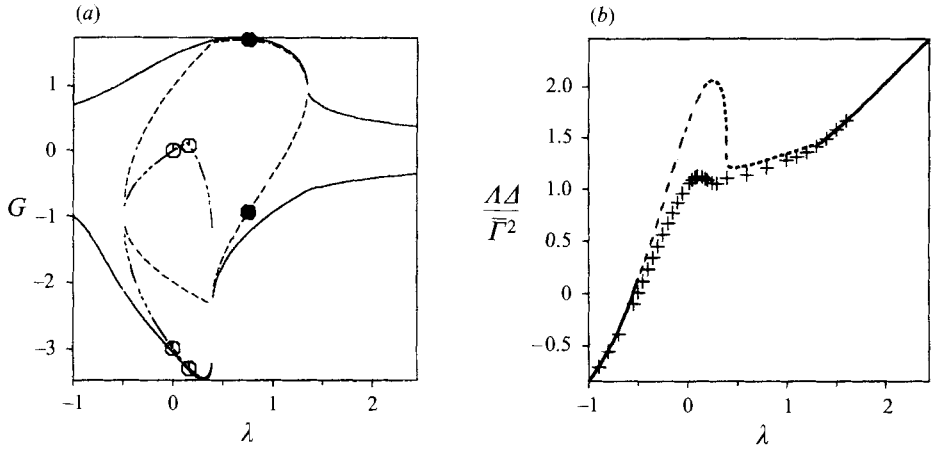

FIGURE 6. (*a*) Signal amplitudes for $A = 5.0$. Maximum and minimum amplitudes (——), compression shock amplitudes (– – –), expansion shock amplitudes (– - - - –). (*b*) Variation of $\Lambda\Delta/\bar{\Gamma}^2$ with λ for $A = 5.0$. Shock curves (– – –), continuous curves (——), viscous solutions (+ + +) ($\bar{\nu} = 0.02$).

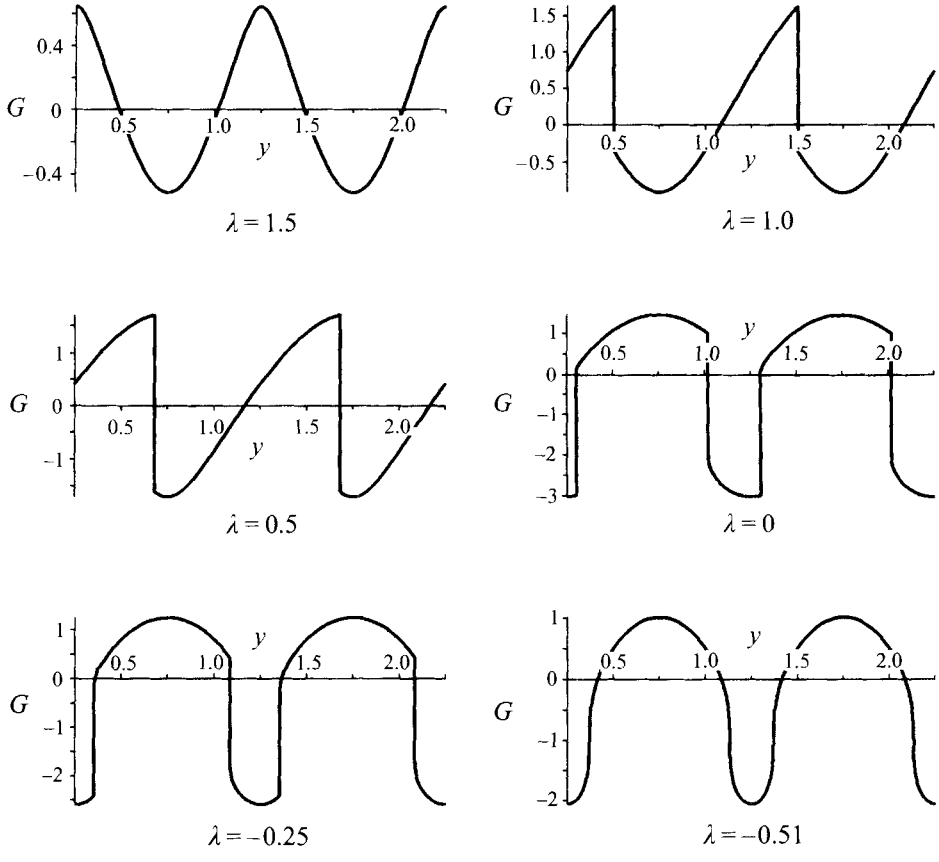

FIGURE 7. Signal profiles for $A = 5.0$.

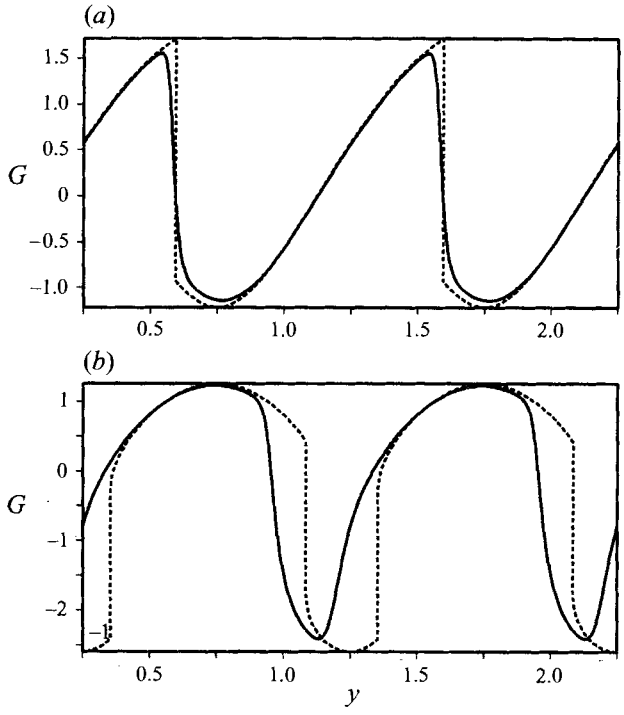

FIGURE 8. Comparison of viscous and inviscid profiles for $A = 5.0$: (*a*) $\lambda = 0.75$, (*b*) $\lambda = -0.25$. Inviscid signal (– – –), viscous signal (——).

$m = 1, h = \frac{1}{3}\sin(2\pi s)$, i.e.

$$\left(\frac{A}{2}g^2 - \delta\right)\frac{\mathrm{d}g}{\mathrm{d}s} + \frac{\pi}{3}\sin(2\pi s) = 0, \qquad \delta = A - \frac{A}{2}\int_{\phi}^{\phi+1} g^2(r)\mathrm{d}r. \tag{5.2}$$

In figure 9(*a*) we give the response curves for $A = 1$. When δ is in the interval $(0, (1/2)^{5/3})$ the signal is discontinuous and consists of two sonic shocks of compression and expansion. Outside this interval the solution is continuous. At $\delta = (1/2)^{5/3}$ the limiting solution as δ is approached from below is different to that when δ is approached from above. This point was made in Chester (1981) analysing a similiar equation arising in the context of a resonating classical gas in an open tube. This is reflected in the response curves of figure 9(*a*) and in the plot of A against δ in figure 9(*b*). Within the context of the model equations presented here the effect of the interaction terms is to make available over most of the frequency range a continuous solution replacing a possible shock solution. The physical frequency range where shocks occur is now extremely small. In figure 10 we give the solution profiles for a range of δ. The resonant band is characterized by sonic shocks. Outside the band the solution is well approximated by linear theory.

6. Conclusions

Resonant gas oscillations have been the subject of intensive study, both from a theoretical and an experimental perspective. This paper provides a small-rate theory for resonant gas oscillations of BZT-fluids. Existing work on BZT-fluids has been concerned exclusively with unidirectional waves in infinite media. This paper

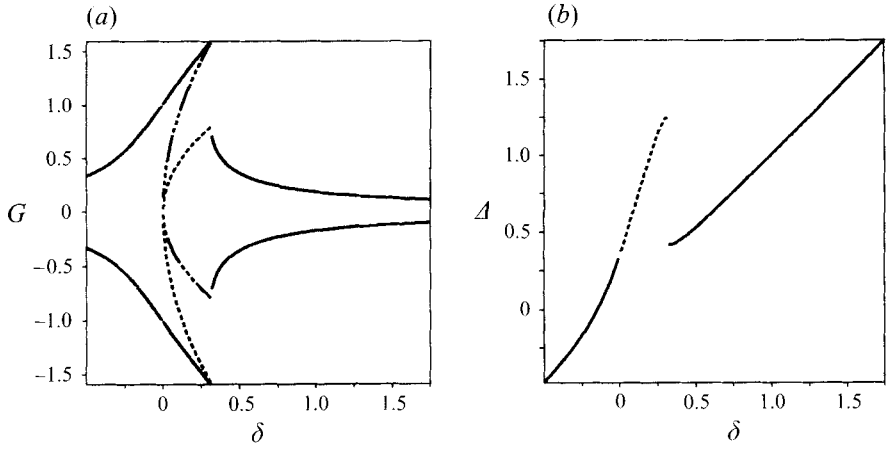

FIGURE 9. (*a*) Signal amplitudes for equation (5.2). Maximum and minimum amplitudes (——). Compression shock amplitudes (– – –). Expansion shock amplitudes (– - – - –). (*b*) Variation of Δ with δ for $\Delta = 1, \bar{\Gamma} = 0$. Shock curves (– – –). Continuous curves (——).

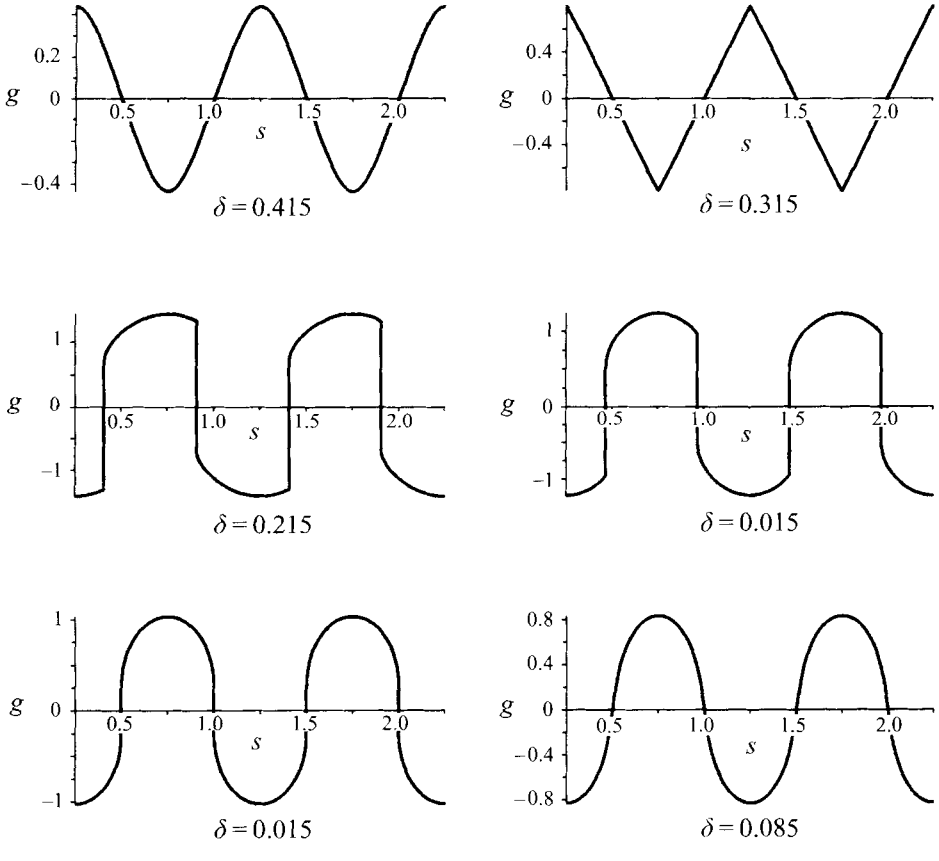

FIGURE 10. Signal profiles for equation (5.2).

represents an extension to waves in finite media where the effect of wave interaction must be included. As such it should provide a basis for future experimental and theoretical investigations.

The theory predicts the existence of a resonant frequency band within which expansion and compression shocks are generated in the signal profiles. An ability to control the strength of shocks produced by frequency detuning, a feature important to the experimentalist, is demonstrated. In contrast to the classical gas case there is an inherent limit on the strength of discontinuities that can propagate within the signal. Within the context of the small-rate theory developed here, discontinuities consistent with the theory (arising from averaged shock conditions) may in fact then exceed strengths sustainable by the propagating signal. These discontinuities are interpreted as approximations to sonic shock and refocused wave fan combinations. Experimental evidence of wave fan disintegration and refocusing within the interior of the gas tube would be expected from this interpretation.

The effective frequency of the resonating system is dependent through wave interaction on the the resonating signal. This results in applied frequency intervals where multiple solutions coexist. That not all these solutions would be observed experimentally is demonstrated in a simple numerical experiment where the resonating system is detuned through the resonant band.

REFERENCES

BETCHOV, R. 1958 Nonlinear oscillations of a column of gas. *Phys. Fluids* **1**, 205–212.

BETHE, H. A. 1942 The theory of shock waves for an arbitary equation of state. *Office Sci. Res. Dev. Rep.* 545.

BORISOV, A. A., BORISOV, AL. A., KUTATELADZE, S. S. & NAKORYAKOV, V. E. 1983 Rarefaction shock wave near the critical liquid vapour point. *J. Fluid Mech.* **126**, 59–73.

CHESTER, W. 1964 Resonant oscillations in closed tubes. *J. Fluid Mech.* **18**, 44–64.

CHESTER, W. 1981 Resonant oscillations of a gas in an open-ended tube. *Proc. R. Soc. Lond.* A **377**, 449–467.

CHESTER, W. & MOSER, A. 1982 On an equation which describes the resonant oscillations of a gas in an open-ended tube. *Proc. R. Soc. Lond.* A **380**, 409–415.

CRAMER, M. S. & BEST, L. M. 1991 Steady isentropic flows of dense gases. *Phys. Fluids* A **3**, 219–226.

CRAMER, M. S. & CRICKENBERGER, A. B. 1991 The dissipative structure of shock waves in dense gases. *J. Fluid Mech.* **223**, 325–355.

CRAMER, M. S. & FRY, R. N. 1993 Nozzle flows of dense gases. *Phys. Fluids* A **5**, 1246–1259.

CRAMER, M. S. & KLUWICK, A. 1984 On the propagation of waves exhibiting both positive and negative nonlinearity. *J. Fluid Mech.* **142**, 9–37.

CRAMER, M. S. & TARKENTON, G. M. 1992 Transonic flows of Bethe–Zel'dovich–Thompson fluids. *J. Fluid Mech.* **240**, 197–228.

CURRAN, H. M. 1981 Use of organic working fluids in Rankine engines. *J. Energy* **5**, 218–223.

DUNN, J. E., FOSDICK, R. & SLEMROD, M. (Ed.) 1993 *Shock induced Transitions and Phase Structures in General Media.* Springer.

FOX, PH. A. 1955 Perturbation theory of wave propagation based on the method of characteristics. *J. Math. Phys.* **34**, 133–151.

JIMENEZ, J. 1973 Nonlinear gas oscillations in pipes. Part 1. Theory. *J. Fluid Mech.* **59**, 23–46.

KLUWICK, A. (Ed.) 1991 *Nonlinear Waves in Real Fluids.* CISM Courses and Lecture Notes vol. 315. Springer.

KLUWICK, A. 1993 Transonic nozzle flow of dense gases. *J. Fluid Mech.* **247**, 661–668.

KLUWICK, A. & SCHEICHL, ST. 1996 Unsteady transonic nozzle flow of dense gases *J. Fluid Mech.* **310**, 113–137

KUTATELADZE, S. S., NAKORYAKOV, V. E. & BORISOV, A. A. 1987 Rarefaction waves in liquid and gas–liquid media. *Ann. Rev. Fluid Mech.* **19**, 577–600.

LIN, C. C. 1954 On a perturbation method based on the method of characteristics. *J. Math. Phys.* **33**, 117–134.

LIU, T. P. 1976*a* The entropy condition and the admissability of shocks. *J. Math. Anal. Appl.* **53**, 78–88.

LIU, T. P. 1976*b* Shock waves in the nonisentropic gas flow. *J. Diffl Equat.* **22**, 442–452.

MORTELL, M. P. & SEYMOUR, B. R. 1979 Nonlinear forced oscillations in a closed tube: continuous solutions of a functional equation. *Proc. R. Soc. Lond.* A **367**, 253–270.

SEYMOUR, B. R. & MORTELL, M. P. 1973*a* Resonant acoustic oscillations with damping: small rate theory. *J. Fluid Mech.* **58**, 353–373

SEYMOUR, B. R. & MORTELL, M. P. 1973*b* Nonlinear resonant oscillations in open tubes *J. Fluid Mech.* **60**, 733–749.

SEYMOUR, B. R. & MORTELL, M. P. 1980 A finite-rate theory of resonance in a closed tube: discontinuous solutions of a functional equation. *J. Fluid Mech.* **99**, 365–382.

SEYMOUR, B. R. & MORTELL, M. P. 1985 The evolution of a finite rate periodic oscillation. *Wave Motion.* **7**, 399–409.

THOMPSON, P. A. 1971 A fundamental derivative in gasdynamics. *Phys. Fluids* **14**, 1843–1849.

THOMPSON, P. A. & LAMBRAKIS, K. C. 1973 Negative shock waves. *J. Fluid Mech.* **60**, 187–207.

ZEL'DOVICH, YA. B. 1946 On the possibility of rarefaction shock waves. *Zh. Eksp. Teor. Fiz.* **4**, 363–364.

ZÖRNER, W. & BLUMENBERG, J. 1989 Der organische Rankine Prozeß zur solardynamischen Energieerzeugung im Weltraum. *Z. Flugwiss. Weltraumforsch* **13**, 260–270.